RET/Papillary Thyroid Carcinoma Oncogenic Signaling through the Rap1 Small GTPase

Valentina De Falco,[1] Maria Domenica Castellone,[1] Gabriella De Vita,[1] Anna Maria Cirafici,[1] Jerome M. Hershman,[2] Carmen Guerrero,[3] Alfredo Fusco,[1] Rosa Marina Melillo,[1] and Massimo Santoro[1]

[1]Istituto di Endocrinologia ed Oncologia Sperimentale del CNR "G.Salvatore", c/o Dipartimento di Biologia e Patologia Cellulare e Molecolare, Universita' Federico II, Naples, Italy; [2]Endocrinology and Metabolism Division, University of California at Los Angeles School of Medicine, Los Angeles, California; and [3]Instituto de Biologia Molecular y Celular del Cancer, Centro de Investigacion del Cancer (Consejo Superior de Investigaciones Científicas-Universidad de Salamanca), University of Salamanca, Salamanca, Spain

Abstract

RET/papillary thyroid carcinoma (PTC) oncoproteins result from the in-frame fusion of the RET receptor tyrosine kinase with protein dimerization motifs encoded by heterologous genes. Here, we show that RET/PTC1 activates the Rap1 small GTPase. The activation of Rap1 was dependent on the phosphorylation of RET Tyr^{1062}. RET/PTC1 recruited a complex containing growth factor receptor binding protein 2–associated binding protein 1 (Gab1), CrkII (v-crk sarcoma virus CT10 oncogene homologue II), and C3G (Rap guanine nucleotide exchange factor 1). By using dominant-negative and small interfering duplex (small interfering RNA) oligonucleotides, we show that RET/PTC1–mediated Rap1 activation was dependent on CrkII, C3G, and Gab1. Activation of Rap1 was involved in the RET/PTC1–mediated stimulation of the BRAF kinase and the p42/p44 mitogen-activated protein kinases. Proliferation and stress fiber formation of RET/PTC1–expressing PC Cl 3 thyroid follicular cells were inhibited by the dominant-negative Rap1(N17) and by Rap1–specific GTPase-activating protein. Thus, Rap1 is a downstream effector of RET/PTC and may contribute to the transformed phenotype of RET/PTC–expressing thyrocytes. [Cancer Res 2007;67(1):381–90]

Introduction

Human papillary thyroid carcinomas (PTC) feature chromosomal aberrations that result in the in-frame fusion of the intracellular kinase domain of the RET receptor with the NH_2 terminus of heterologous proteins, generating the RET/PTC oncoproteins (1, 2). RET/PTC1 (the H4-RET fusion) and RET/PTC3 (the NCOA4-RET fusion) are the most prevalent variants. Fusion with protein partners possessing protein-protein interaction motifs provides RET/PTC kinases with dimerizing interfaces, thereby resulting in ligand-independent autophosphorylation and signaling. Among the autophosphotyrosines, Y1062 plays an important role in RET-mediated cell transformation (3–6). Accordingly, when phosphorylated, it acts as the binding site for several protein tyrosine binding–containing proteins, including Src homology and collagen (Shc), insulin receptor substrate 1/2, fibroblast growth factor receptor substrate 2 (FRS2), and downstream of kinase 1/4/5 (7). Binding to Shc and FRS2 mediates recruitment of growth factor receptor binding protein 2 (Grb2)/SOS complexes so leading to GTP exchange and Ras stimulation (7, 8). This results in the activation of the BRAF serine/threonine kinase (6, 9, 10). Docking proteins that bind Tyr^{1062} are also able to mediate RET binding to Grb2-associated binding protein (Gab) family adaptors (Gab1 and Gab2; refs. 8, 11, 12). Gab1/2 are large docking proteins able to associate to many SH2 or SH3 domain–containing proteins, including Grb2, p85, PLCγ, Shc, Shp2, and Crk (13).

Rap1 is a member of the Ras family of small G proteins (14, 15). Although it was initially isolated as a Ras inhibitor (and called KREV for K-Ras revertant; ref. 16), subsequent studies have shown that Rap1, like Ras, can activate the extracellular signal-regulated kinase (ERK) cascade at least in some cell types (14, 17–20). Ras and Rap1 bind to common effectors, including RAF, BRAF, and RalGDS (14). Moreover, Rap1 signaling leads to integrin activation, F-actin fiber formation, and cell adhesion (14, 15). Recently, it has been shown that Rap1b has mitogenic activity in rat thyroid cells (21). However, microinjection of the Rap1 protein failed to induce proliferation of dog thyrocytes showing that Rap1 alone is not sufficient to trigger thyroid cell growth (22); no mutations in Rap1 have been found in thyroid follicular adenomas (23). Here, we show that RET/PTC1 activates Rap1 in a Tyr^{1062}-dependent fashion and we provide evidence that Rap1 is required for RET/PTC1–induced BRAF activation, mitogenesis, and actin cytoskeleton rearrangement.

Materials and Methods

Cell lines. HEK293 cells were grown in DMEM supplemented with 10% FCS (Invitrogen Groningen, the Netherlands). Transient transfections were carried out with the LipofectAMINE reagent according to the manufacturer's instructions (Invitrogen). PC Cl 3 (PC) were cultured in Coon's modified Ham's F12 medium supplemented with 5% calf serum and a mixture of six hormones, including thyrotropin (10 mU/mL), hydrocortisone (10 nmol/L), insulin (10 μg/mL), apotransferrin (5 μg/mL), somatostatin (10 ng/mL), and glycyl-histidyl-lysine (10 ng/mL; Sigma Chemical Co., St. Louis, MO; ref. 6). PC RET/PTC1, PC RET/PTC1(Y1062F), and PC BRAF(V600E) cells have been described previously (6). For stable transfections, 5×10^5 cells were plated 48 h before transfection in 60-mm tissue culture dishes. Calcium phosphate DNA precipitates were incubated with the cells for 1 h. Cells were then incubated with 15% glycerol in HEPES-buffered saline for 2 min. Mass populations of several cell clones and single clones were obtained by puromycin (2 μg/mL) selection. The PC cell line expressing RET/PTC1 in a doxycyline-dependent manner was a kind gift of Dr. J.A. Fagin (Memorial Sloan-Kettering Cancer Center, New York, NY; ref. 24). To induce RET/PTC expression, cells were treated for different times

Note: V. De Falco and M.D. Castellone contributed equally to the work.

Requests for reprints: Massimo Santoro, Dipartimento di Biologia e Patologia Cellulare e Molecolare, Medical School, University "Federico II" of Naples, via Sergio Pansini 5, 80131 Naples, Italy. Phone: 39-081-7463056; Fax: 39-081-7463037; E-mail: masantor@unina.it.

doi:10.1158/0008-5472.CAN-06-0981

with 1 μg/mL doxycycline. The RET/PTC1–positive TPC1, FB2, BHP2-7, and BHP10-3 human PTC cell lines and the P5 primary culture of normal human thyroid follicular cells were grown as described elsewhere (25).

Plasmids. All the RET constructs used in this study were cloned in pCDNA3.1(Myc-His) (Invitrogen); they encode the short (RET-9) RET spliced form (6). For simplicity, we numbered the residues of RET/PTC proteins as the corresponding residues in unrearranged RET. Briefly, RET/PTC1(K−) is a kinase-dead mutant, carrying the substitution of the Lys^{758} with a methionine. RET/PTC1(Y1062F) carries the substitution of the indicated tyrosine with phenylalanine. Plasmids encoding Rap1 (Rap1a), the constitutively active Rap1(V12), the dominant-negative Rap1(N17), Rap1–specific GTPase-activating protein (Rap1GAP), AU5-tagged constitutively activated Rho(QL), and Ras(V12) were kind gifts of J.S. Gutkind (NIH, Bethesda, MD). Long Terminal Repeat 2 (LTR2) vectors encoding full-length C3G and C3GΔCAT mutant, lacking the COOH-terminal half of the protein (last 457 bp), are described elsewhere (26). The pcDNA3 expression vector encoding Gab1 was a kind gift of P. Gual and S. Giordano (Instituto per la Ricerca e la Cura del Cancro, Candiolo, Torino, Italy; ref. 27). The pCMV6-CrkII plasmid was from OriGene Technologies, Inc. (Rockville, MD). The plasmid encoding the myc-tagged isolated SH2 domain of CrkII (residues 13–118; SH2CrkII) was obtained by PCR and subcloning into pCDNA3.1 (Myc-His). The plasmid encoding enhanced green fluorescent protein (pEGFP) was from Clontech (Mountain View, CA).

Antibodies. Anti-RET is an affinity-purified polyclonal antibody raised against the tyrosine kinase protein fragment of human RET. Anti–phospho-p44/42 mitogen-activated protein kinase (MAPK), specific for MAPK (ERK1/2) phosphorylated at Thr^{202}/Tyr^{204}, anti–p44/42 MAPK, anti–phospho-MAPK/ERK kinase (MEK) 1/2, specific for MEK1 and MEK2 phosphorylated at Ser^{217}/Ser^{221}, and anti-MEK1/2 were from Cell Signaling (Beverly, MA). Anti-Rap1, anti-myc antibody, anti-C3G (C-19), anti-BRAF, anti-CrkII, and anti-RhoA were from Santa Cruz Biotechnology (Santa Cruz Biotechnology, CA). Anti-Gab1, anti-phosphotyrosine, and anti-Ras (clone 10) antibodies were from Upstate Biotechnology, Inc., (Lake Placid, NY). Monoclonal anti-AU5 (MMS135R) was from BAbCO (Berkeley Antibody Co., Inc., Richmond CA). Monoclonal anti-α tubulin was from Sigma Chemical. Secondary antibodies coupled to horseradish peroxidase were from Amersham Pharmacia Biotech (Little Chalfort, United Kingdom).

Protein studies. Protein extractions and immunoblotting experiments were done according to standard procedures. Immune complexes were detected with the enhanced chemiluminescence kit (Amersham). Signal intensity was analyzed at the PhosphorImager (Typhoon 8600, Amersham Pharmacia Biotech) interfaced with the ImageQuant software.

BRAF kinase assay. The BRAF kinase assay was done as described previously (6). Briefly, HEK293 cells were transiently transfected with the indicated vectors, cultured for 18 h in serum-deprived medium, and harvested. BRAF kinase was immunoprecipitated with the anti-BRAF antibody and resuspended in a kinase buffer containing 100 mmol/L $MgCl_2$, 20 μmol/L ATP, and 0.5 μg of recombinant glutathione *S*-transferase (GST) MEK (Upstate Biotechnology). After a 15-min incubation at 30°C, reactions were stopped by adding 2× Laemmli buffer. Proteins were then subjected to 10% SDS gel electrophoresis and immunoblotted with anti–phospho-MEK1/2 antibodies.

Small GTPases activity assays. Small GTPases activity assays were done as described elsewhere (28). Briefly, cells were serum starved for 8 h and lysed at 4°C in a buffer containing 20 mmol/L HEPES (pH 7.4), 0.1 mol/L NaCl, 1% Triton X-100, 10 mmol/L EGTA, 40 mmol/L β-glycerophosphate, 20 mmol/L MgCl2, 1 mmol/L Na_3VO_4, 1 mmol/L DTT, 10 μg/mL aprotinin, 10 μg/mL leupeptin, and 1 mmol/L phenylmethylsulfonyl fluoride. Lysates were incubated for 30 min with glutathione sepharose beads coupled to GST fusion proteins containing either the Rap1-binding domain (RalGDS), the Ras-binding domain (RafRBD), or the Rho-binding domain (GST-RhotekinGDS). Total Rap1, Ras, and RhoA levels and levels of their GTP-loaded forms (bound to GST-fusion proteins) were determined by immunoblot.

Cell growth and staining. For growth curves, 0.5×10^5 cells were seeded in complete medium and counted at the indicated time points. DNA synthesis was measured by the bromodeoxyuridine (BrdUrd) labeling and detection kit from Boehringer Mannheim (Germany).

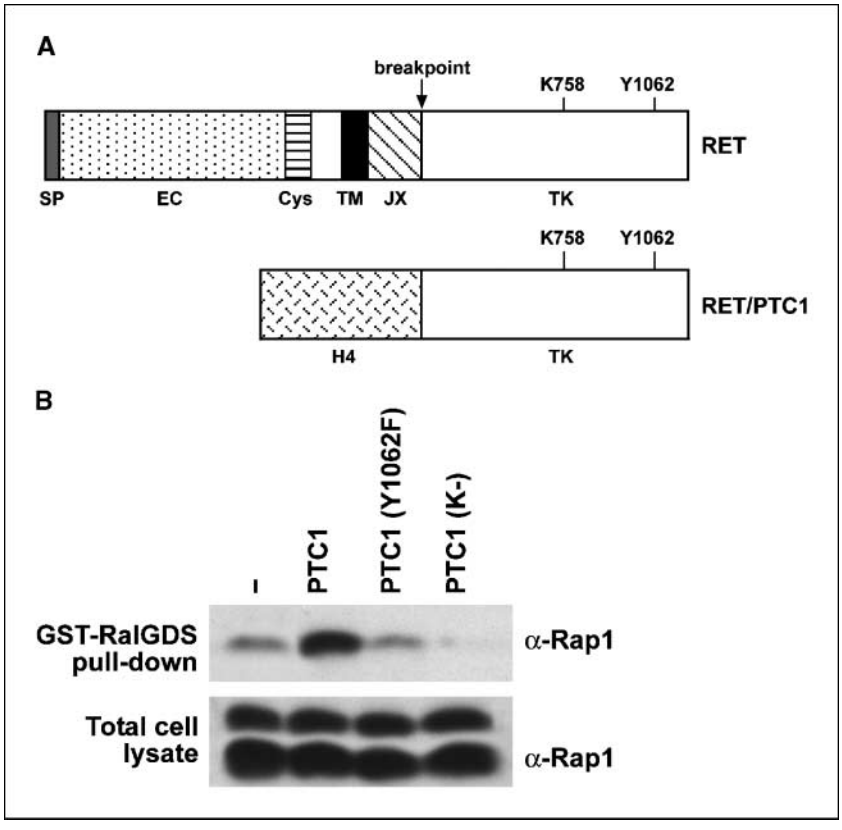

Figure 1. *A,* schematic representation of the RET/PTC1 constructs used in this study. *SP,* RET signal peptide; *EC,* extracellular domain; *Cys,* cysteine rich, *TM,* transmembrane; *JX,* juxtamembrane; *TK,* tyrosine kinase. RET/PTC breakpoint. RET Tyr^{1062} (corresponding to Y451 in RET/PTC1) and Lys^{758} (corresponding to K147 in RET/PTC1). *B,* affinity precipitation of Rap1 with immobilized GST-RalGDS fusion protein from HEK293 transfected with the indicated RET/PTC1 constructs or the empty vector (−). Bound Rap1 was revealed by staining blot with anti-Rap1 (α-*RAP1*). Total Rap1 levels are shown for normalization. The signal was analyzed at the PhosphorImager. This experiment is representative of at least four independent assays.

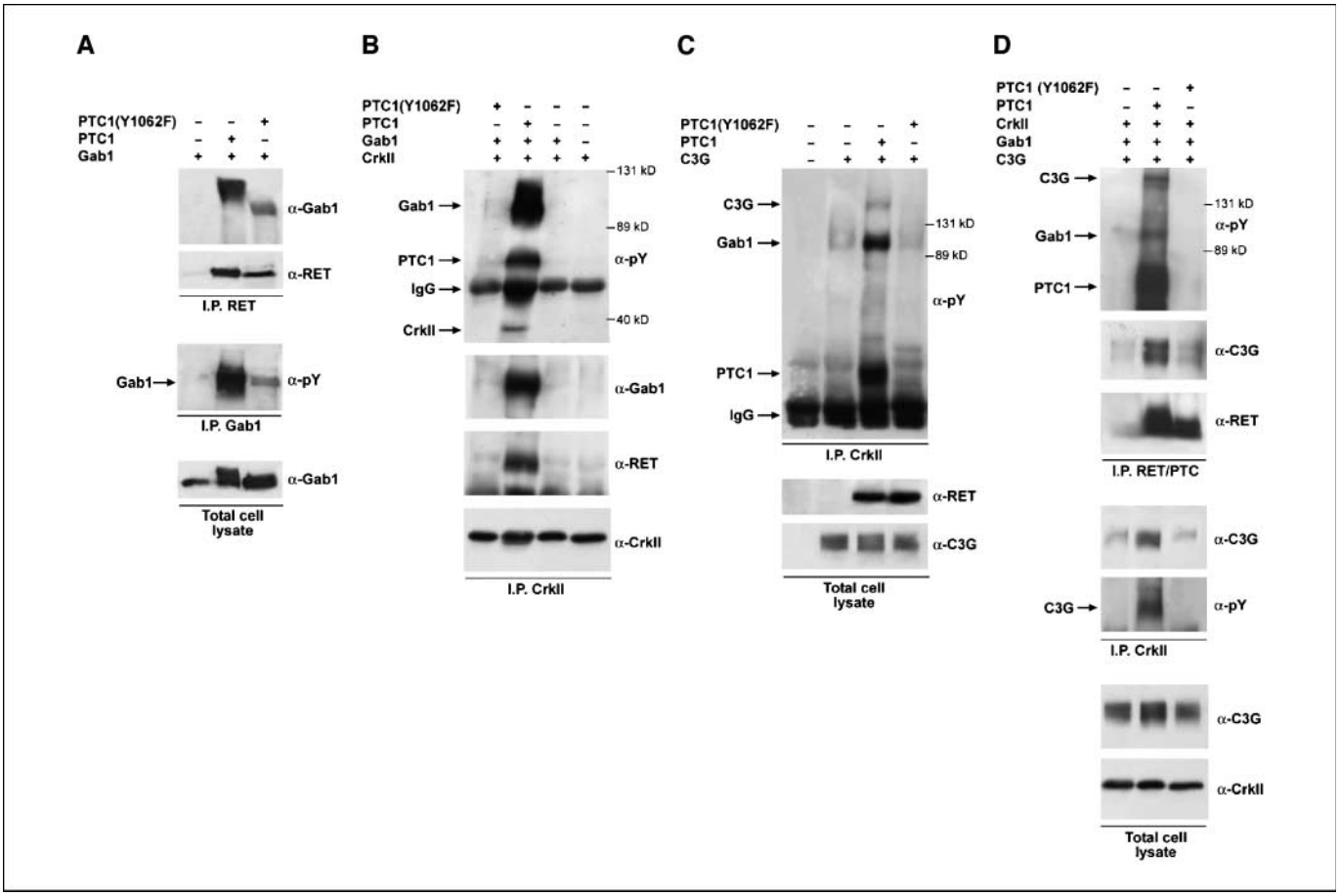

Figure 2. *A,* protein lysates (500 μg) from HEK293 transfected with Gab1 and the indicated RET/PTC plasmids were immunoprecipitated (*I.P.*) with anti-RET (α-*RET*) and immunoblotted with anti-Gab1 (α-*Gab1*) or anti-RET for normalization (*top*). Alternatively, protein lysates were immunoprecipitated with anti-Gab1 and immunoblotted with anti-phosphotyrosine (α-*pY*) antibodies (*middle*). Total Gab1 levels were determined for normalization (*bottom*). *B,* CrkII coimmunoprecipitated with tyrosine-phosphorylated RET/PTC1 and Gab1. Protein lysates (500 μg) from HEK293 transfected with CrkII, and where indicated Gab1 and RET/PTC1, were immunoprecipitated with anti-CrkII (α-*CrkII*) and immunoblotted with anti-phosphotyrosine. RET/PTC1 and Gab1 were identified by reprobing with specific antibodies. CrkII levels are shown for normalization. *C,* protein lysates (2 mg) from HEK293 transfected with RET/PTC1 or its mutant Y1062F were immunoprecipitated with anti-CrkII and immunoblotted with anti-phosphotyrosine. RET/PTC1 and Gab1 were identified by reprobing with specific antibodies (data not shown). *D,* RET/PTC1–stimulated CrkII-C3G binding. Protein lysates (500 μg) from HEK293 transfected with the indicated plasmids, in the presence or not of RET/PTC1, were immunoprecipitated with anti-RET and blotted with phosphotyrosine, C3G, or RET (*top*) or immunoprecipitated with anti-CrkII and immunoblotted with C3G or phosphotyrosine antibodies (*middle*). Total cell lysates were immunoblotted for normalization (*bottom*). These findings are representative of several independent assays.

Briefly, cells were seeded on glass coverslips, incubated for 1 h with BrdUrd (final concentration of 10 μmol/L), fixed, and permeabilized with ethanol-glycine solution. Coverslips were incubated with anti–BrdUrd mouse monoclonal antibody and with a rhodamine-conjugated secondary antibody (Jackson ImmunoResearch Laboratories, Philadelphia, PA) and mounted in Moviol on glass slides. Cell nuclei were identified by Hoechst 33258 (final concentration of 1 μg/mL; Sigma Chemical) staining. The fluorescent signal was visualized with an epifluorescent microscope (Axiovert 2, Zeiss; equipped with a ×100 lens) interfaced with the image analyzer software KS300 (Zeiss). At least 100 GFP-positive cells were counted in five different microscopic fields. For actin staining, cells were seeded on glass coverslips, fixed with paraformaldeyde (4%), and permeabilized with Triton X-100 (0.2%). Actin rearrangements were revealed by treating coverslips with Texas Red X–conjugated phalloidin (Molecular Probes) for 1 h. For transient experiments, cells were transiently transfected as described above. Briefly, various combinations of plasmids were cotransfected with pEGFP in a 1:10 ratio. After 36 h, cells were plated, fixed at different time points, and stained. All coverslips were counterstained with PBS containing Hoechst 33258 and analyzed with an epifluorescent microscope (Axiovert 2). Experiments were done in triplicate and at least 60 EGFP-positive cells were scored for each transfection. To assess statistical significance, Bonferroni multiple comparison test was applied and the Instat software program (GraphPad Software, Inc.) was used. Differences were significant at $P < 0.01$.

Reporter assay. The pSRF-luc plasmid contains the luciferase (*Firefly* luciferase) reporter gene driven by a basic promoter element (TATA box) joined to tandem repeats of serum responsive factor (SRF) binding elements (Stratagene, La Jolla, CA; ref. 29). HEK293T cells were transfected with the required expression vector together with 0.1 μg of the pSRF-luc reporter and 0.01 μg phRL, which expresses *Renilla* luciferase from *Renilla* reniformis for normalization. The total amount of plasmid DNA was adjusted with pcDNA3–β-galactosidase. *Firefly* and *Renilla* luciferase activities were assayed using the Dual-Luciferase Reporter System (Promega Corp., Madison, WI). Light emission was quantitated using a Berthold Technologies luminometer (Centro LB 960). Experiments were done in triplicate and data were represented as average ± SD.

RNA silencing. Small inhibitor duplex RNAs targeting Gab1 were as described elsewhere (30) and were chemically synthesized by Proligo (Boulder, CO). The scrambled control oligonucleotide was 5′-AGGAUAGC-GUGGAUUUCGGUTT-3′. For small interfering RNA (siRNA) transfection, cells were grown under standard conditions. The day before transfection,

cells were plated in six-well dishes at 30% to 40% confluency. Transfection was done using 5 μg of duplex RNA and 6 μL Oligofectamine reagent (Invitrogen). Cells were harvested 48 h after transfection.

Results

RET/PTC1 activates Rap1 in a kinase- and Y1062-dependent manner. Vectors expressing wild-type (WT) and mutant RET/PTC1 were transiently transfected with Rap1 into HEK293 cells. The RET/PTC1 mutants used were the kinase dead PTC1(K−) mutant and the Tyr^{1062} to phenylalanine PTC1(Y1062F) mutant (Fig. 1*A*). Protein lysates were pulled down with GST-RalGDS, which binds specifically to GTP-loaded activated Rap1. Immunoblotting with anti-Rap1 revealed that Rap1 activity was stimulated by RET/PTC1 (>5-fold; Fig. 1*B*). Rap1 stimulation required RET/PTC1 kinase activity as well as Tyr^{1062} (Fig. 1*B*).

A Gab1-CrkII-C3G complex mediates RET/PTC1–induced Rap1 activation. Rap1 is activated by numerous guanine nucleotide exchange factors (GEF), such as C3G, cyclic AMP–GEFs (Epac), CalDAG-GEF, and PDZ-GEF (14, 15). C3G forms a complex with the Crk adaptor proteins by binding to the NH_2-terminal SH3 domain of Crk (31). The C3G-Crk complex is activated via the interaction between the Crk SH2 domain and phosphotyrosines. The Gab1 docking protein contains six potential binding sites for the SH2 of Crk (31, 32). Because it has been reported that RET binds to Gab1 (8, 11, 12), we hypothesized that Gab1, Crk, and C3G may be involved in RET/PTC1–mediated Rap1 activation. Coexpression of RET/PTC1 and Gab1 in HEK293 cells followed by RET/PTC immunoprecipitation and Gab1 immunoblot showed that the two proteins interacted *in vivo* (Fig. 2*A, top*). Gab1 immunoprecipitation and phosphotyrosine immunoblot showed that the binding resulted in Gab1 phosphorylation (Fig. 2*A, middle*) and mobility shift (Fig. 2*A*). RET/PTC1-Gab1 binding was dependent on the integrity of Tyr^{1062} because the amount of coimmunoprecipitated Gab1 (Fig. 2*A, top*), its mobility shift (Fig. 2*A, top*), and its tyrosine phosphorylation levels (Fig. 2*A, middle*) were affected by the Y1062F mutation.

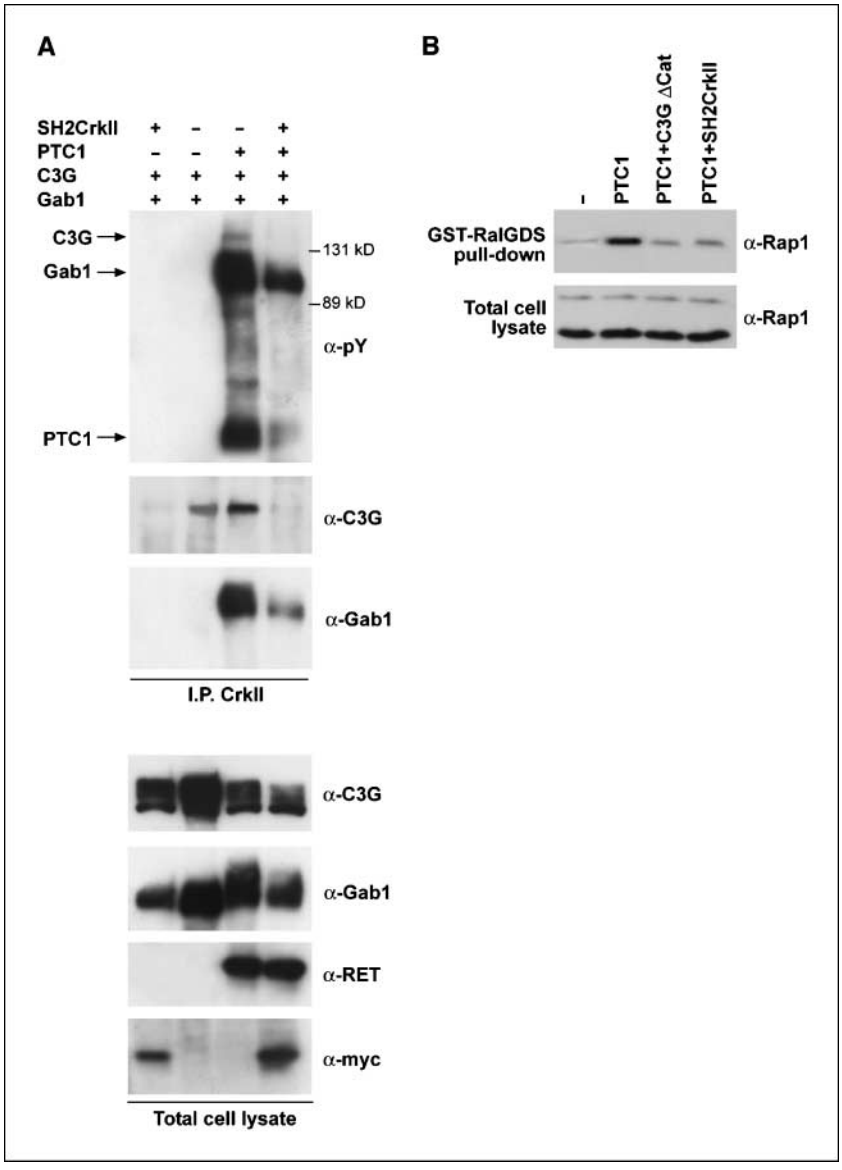

Figure 3. *A,* cells were transfected with C3G and Gab1 and other plasmids where indicated. Proteins were immunoprecipitated with CrkII and blotted with the indicated antibodies (*top*). Total cell lysates were immunoblotted with C3G, Gab1, and RET antibodies for normalization. Anti-myc (tag) was used for SH2CrkII (*bottom*). *B,* Rap1 was affinity precipitated with immobilized GST-RalGDS. Bound Rap1 was revealed by immunoblot. These findings are representative of several independent assays.

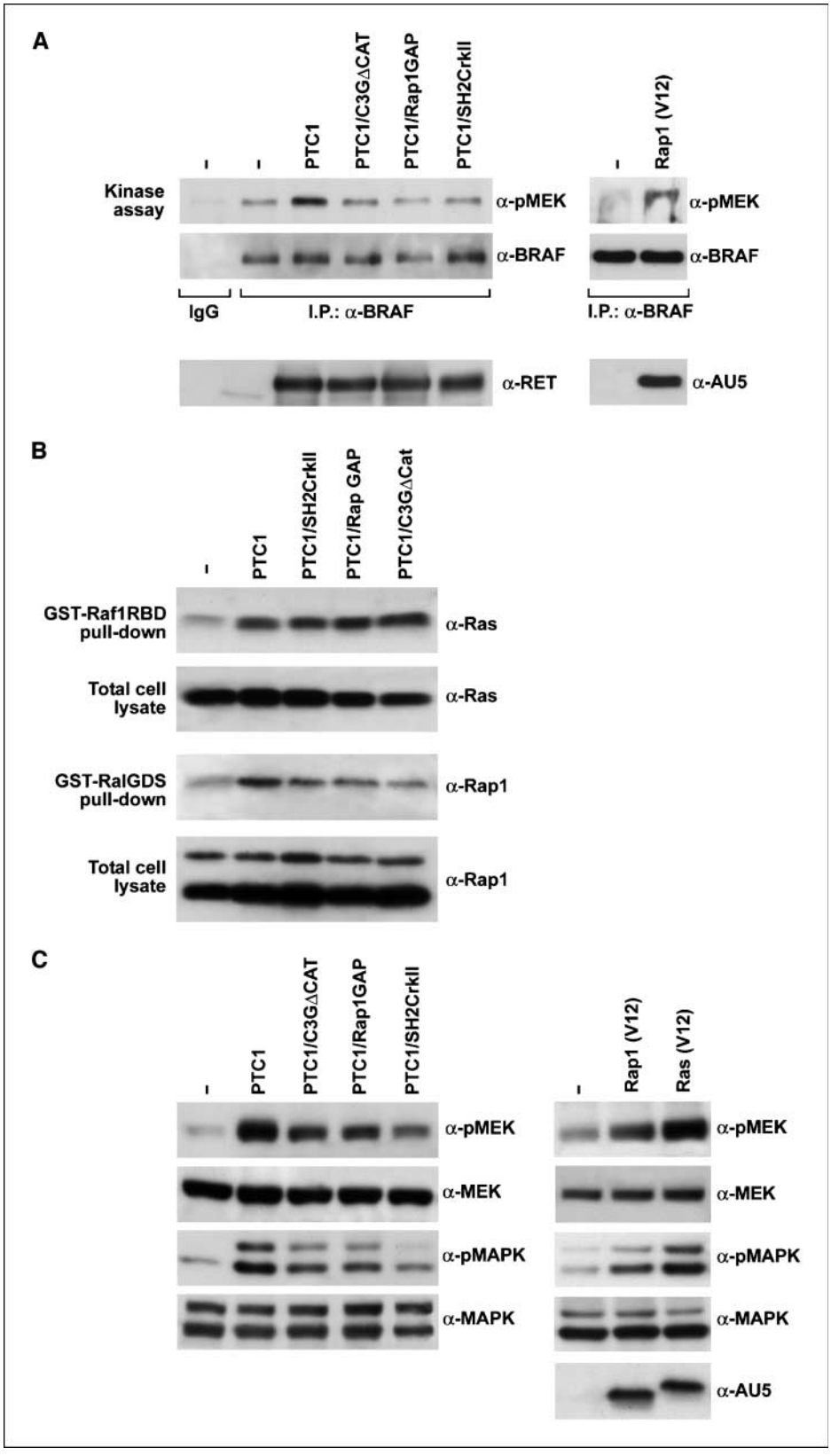

Figure 4. *A,* HEK293 were transfected with the indicated plasmids, kept overnight in serum-deprived medium, and harvested. Cell lysates were subjected to an *in vitro* BRAF kinase assay using GST-MEK as a substrate. Kinase reactions were analyzed with anti–phospho-MEK (α-*pMEK*) antibody. Filters were reprobed with anti-BRAF (α-*BRAF*). Total cell extracts were immunoblotted with anti-RET or with anti-AU5 (α-*AU5*; the Rap1 tag) for normalization. *B,* HEK293 were transfected with RET/PTC1 and the indicated plasmids. Rap1 or Ras activity was measured by precipitation with GST-RalGDS or GST-RafRBD, respectively. Total Rap1 and Ras levels are shown for normalization. The signal was analyzed at the PhosphorImager. *C,* MEK and MAPK phosphorylation was evaluated in HEK293 cells transfected with the indicated plasmids by immunoblotting with phosphospecific antibodies. The AU5 tag (Rap1 and Ras constructs) was used for normalization. The experiments are representative of at least three independent assays.

Then, HEK293 cells were cotransfected with Gab1, CrkII, and RET/PTC1. Protein lysates were immunoprecipitated with anti-CrkII antibodies and blotted with phosphotyrosine (Fig. 2*B*). The various phosphorylated bands coprecipitated with CrkII were identified by subsequent reprobing of the filter with Gab1 and RET antibodies. CrkII coprecipitated with tyrosine-phosphorylated Gab1 and RET/PTC1. As expected, the complex did not form in the absence of RET/PTC1 or in the presence of the RET/

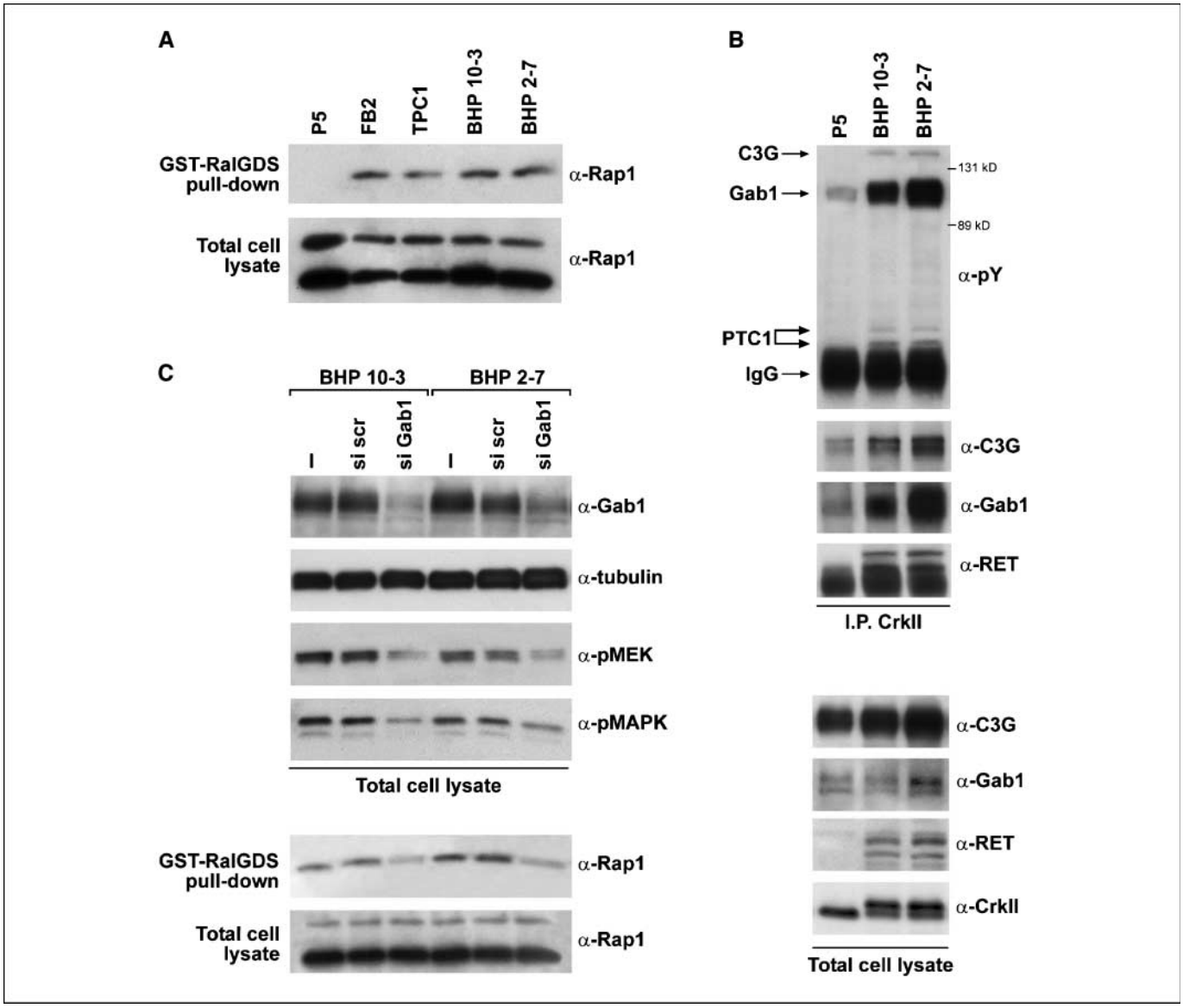

Figure 5. *A,* GST-RalGDS pull-down assay of Rap1 in RET/PTC1–expressing cells compared with normal P5 cells. *B,* RET-PTC1-Gab1-CrkII-C3G complex in thyroid cancer cells. Total lysates (4 mg) of the indicated cell lines were immunoprecipitated with CrkII and blotted with the indicated antibodies. *C,* si Gab1 or control si scr were transiently transfected in the indicated cells. Gab1 levels were measured by immunoblot (*top*); levels of MEK and MAPK phosphorylation were measured by immunoblot (*middle*); Rap1 activation was measured by the GST-RalGDS pull-down assay (*bottom*).

PTC1(Y1062F) mutant (Fig. 2*B*). Thus, HEK293 cells were transfected only with RET/PTC1, and protein lysates were immunoprecipitated with anti-CrkII and blotted with phosphotyrosine. The protein complex was detectable also when Gab1 and CrkII were expressed at endogenous levels (Fig. 2*C*).

HEK293 cells were transfected with CrkII alone or together with RET/PTC1 and C3G. As shown in Fig. 2*D*, a complex containing tyrosine-phosphorylated C3G and Gab1 was formed on WT RET/PTC1 but not on the Y1062F mutant (Fig. 2*D, top*). By immunoprecipitating CrkII, we could show that C3G complexed with CrkII constitutively and that this interaction was enhanced in the presence of RET/PTC1 (Fig. 2*D, middle*).

We used a dominant-negative plasmid encoding the isolated myc-tagged CrkII-SH2 domain (SH2CrkII). HEK293 cells were cotransfected with Gab1 and C3G and, where indicated, RET/PTC1 and the SH2CrkII plasmid. Protein lysates were immunoprecipitated with an anti-CrkII that does not react with its SH2 domain and blotted with phosphotyrosine, C3G, or Gab1 antibodies. The expression of SH2CrkII decreased the amount of both Gab1 and RET/PTC1 coimmunoprecipitated with endogenous CrkII (Fig. 3*A*). In addition, C3G binding to endogenous CrkII decreased in the presence of SH2CrkII (Fig. 3*A*).

Finally, to investigate whether both CrkII and C3G were required for RET/PTC1–induced Rap1 activation, we used the isolated SH2CrkII domain and C3GΔCAT, a C3G mutant devoid of the GEF activity. In the presence of RET/PTC1, the amount of active Rap1 precipitated with GST-RalGDS was clearly inhibited by both SH2CrkII and C3GΔCAT (Fig. 3*B*).

Rap1 is involved in RET/PTC1–induced BRAF/MAPK activation. RET/PTC activates the MAPKs (p42/p44 ERKs) through its

Tyr[1062] and BRAF activation (6). We reasoned that although BRAF activation by RET/PTC was dependent on Ras (6), it was possible that Rap1 contributed to this activation as well. To verify this possibility, we did *in vitro* BRAF kinase assays. As shown in Fig. 4*A*, the activity of BRAF increased in HEK293 cells transfected with RET/PTC1. BRAF stimulation was blunted when RET/PTC1 was coexpressed with Rap1GAP, SH2CrkII, or C3GΔCAT (Fig. 4*A*). As a control, Rap1(V12) expression was also able to stimulate BRAF (Fig. 4*A*). To exclude that the overexpression of Rap1GAP, SH2CrkII, or C3GΔCAT exerted off-target effects on Ras that may in turn be responsible for BRAF inhibition, we also controlled GTP loading on Ras by pull down with GST-RafRBD. Ras activation by RET/PTC was not affected by Rap1GAP, SH2CrkII, or C3GΔCAT expression (Fig. 4*B*).

MEK and MAPK activation by RET/PTC1 was measured with phosphospecific antibodies. Phosphorylation was reduced but not abrogated by the coexpression of Rap1GAP, SH2CrkII, or C3GΔCAT

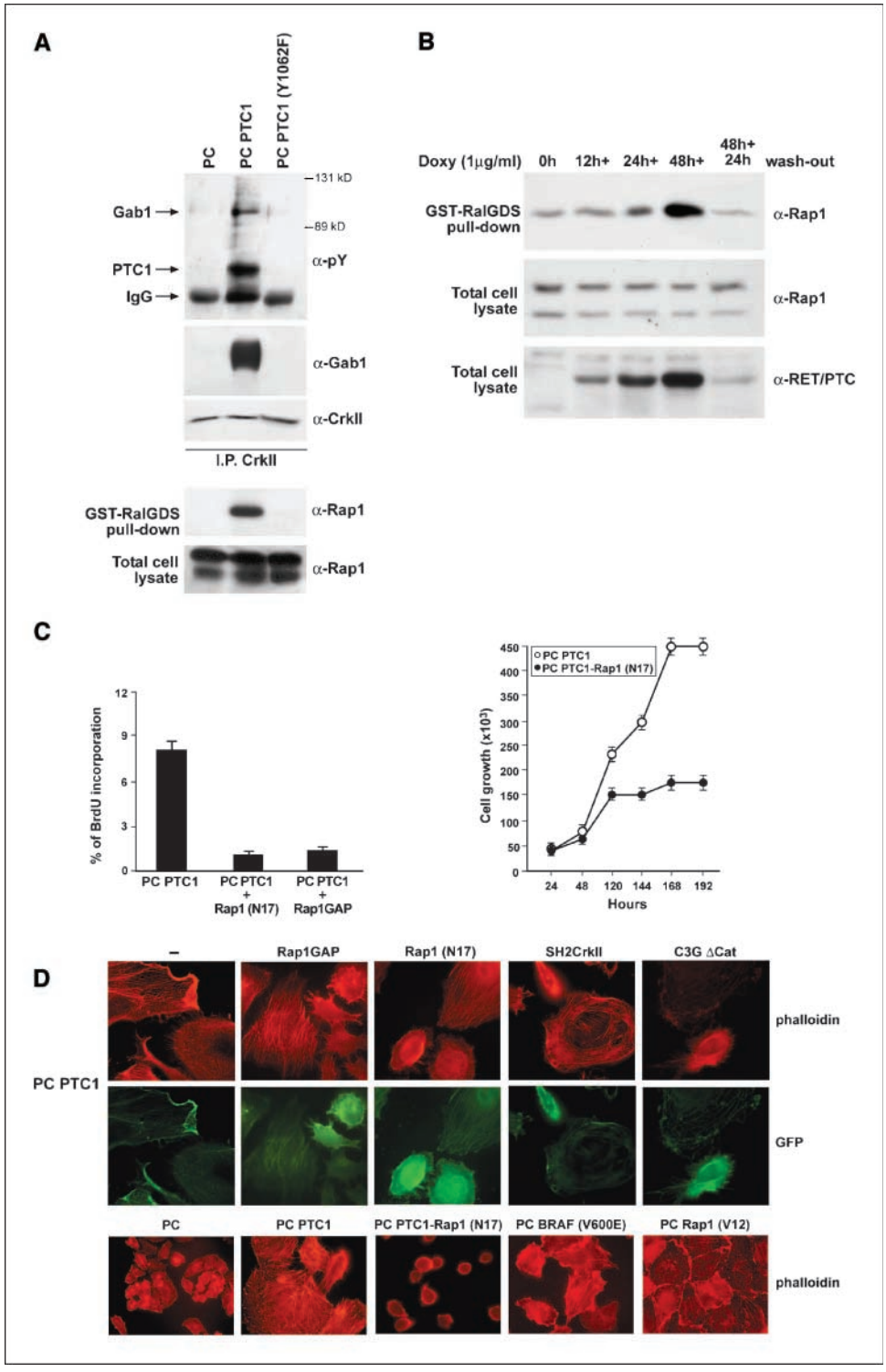

Figure 6. *A,* total lysates (2 mg) of PC cells stably transfected with RET/PTC1 or its Y1062F mutant were immunoprecipitated with CrkII and blotted with the indicated antibodies (*top*). Rap1 activity was measured by the GST-RalGDS pull-down assay in RET/PTC1 or RET/PTC1(Y1062F) transfectants (*bottom*). *B,* PC cells expressing a doxycycline-responsive RET/PTC1 were stimulated with doxycycline and harvested at the indicated time points. Cell lysates were subjected to the GST-RalGDS affinity precipitation. *C,* RET/PTC1–expressing PC cells were transiently transfected with the indicated plasmids together with EGFP. Cells were kept in the absence of six hormones. BrdUrd incorporation was evaluated in EGFP-positive cells; at least 100 cells were counted per field. *Columns,* average of three independent experiments, in which at least 500 cells were scored; *bars,* SD (*left*). PC PTC1 and PC PTC1-Rap1(N17) cells were plated at the same density, kept in the absence of six hormones, and counted at the indicated time points. *Points,* average results of three independent determinations; *bars,* SD (*right*). *D,* PC PTC1 cells were transiently cotransfected with the indicated dominant interfering mutants and EGFP; 36 h after transfection, cells were plated and stained after 4 h with Texas Red X–conjugated phalloidin. Actin organization in EGFP-positive cells was evaluated. Representative fields. The experiment was done in triplicate and at least 60 EGFP-positive cells were scored (*top*). The indicated stable transfectants were fixed with paraformaldehyde (4%) and stained with Texas Red X-conjugated phalloidin (*bottom*).

(Fig. 4*C, left*). This was consistent with the possibility that mutiple pathways (including Rap1 and Ras) lead to BRAF/MAPK stimulation by RET/PTC. Thus, we compared the relative contribution of Ras and Rap1 on MEK/MAPK phosphorylation. As shown in Fig. 4*C* (*right*), both Rap1(V12) and Ras(V12), when transiently expressed in HEK293 cells, were able to trigger MEK and MAPK phosphorylation, with Ras(V12) being ~2-fold more active than Rap1(V12).

Rap1 activation in RET/PTC–positive human thyroid cancer cells. We used human thyroid papillary carcinoma cell lines endogenously expressing RET/PTC1 (FB2, TPC1, BHP2-7, and BHP10-3). High levels of Rap1 activation were found in RET/PTC1–positive cell lines compared with a primary culture of normal thyroid cells (P5; Fig. 5*A*). We could also show, by immunoprecipitating CrkII and blotting with C3G, Gab1, and RET antibodies, that a RET/PTC1-Gab1-CrkII-C3G protein complex was present in the RET/PTC1–positive cell lines (Fig. 5*B*). Small interfering duplex oligonucleotides (si Gab1) were used to knock down Gab1 expression. The transfection in BHP10-3 and BHP2-7 cells of the Gab1 siRNA, but not of the scrambled control (si scr), resulted in the suppression of Rap1 activation (Fig. 5*C, bottom*) and MEK/MAPK phosphorylation (Fig. 5*C, top*).

Rap1 is required for cell growth and stress fiber formation in RET/PTC1–expressing thyrocytes. PC, a continuous line of follicular thyroid cells, requires a mixture of six hormones, including thyrotropin, for proliferation. RET/PTC1 expression in these cells induces hormone-independent proliferation in a Y1062-dependent manner (6). We verified whether the pathway described above was active in PC cells. Figure 6*A* (*top*) shows that in PC cells stably expressing RET/PTC1 (PC PTC1), but not in those expressing the Y1062F mutant, endogenous CrkII and Gab1 coimmunoprecipitated with RET/PTC1. Furthermore, Fig. 6*A* (*bottom*) shows that Rap1 activity, assessed by the GST-RalGDS pull-down assay, was increased in RET/PTC1–expressing cells but not in RET/PTC1(Y1062F)-expressing cells. Thus, we used a PC cell line, in which the expression of RET/PTC1 was under the control of a doxycyline-dependent promoter (24). As shown in Fig. 6*B*, Rap1 activation followed doxycyline-induced RET/PTC1 expression, and peaked at 48 h, when RET/PTC1 levels were the highest. The washout of doxycycline decreased both RET/PTC1 expression and Rap1 activation (Fig. 6*B*).

PC PTC1 cells were cotransfected with plasmids encoding Rap1GAP or the dominant-negative Rap1(N17) together with trace amounts of EGFP to track transfected cells. BrdUrd incorporation was assessed by epifluorescence to monitor DNA synthesis rate in the absence of thyrotropin. As shown in Fig. 6*C*, both Rap1(N17) and Rap1GAP exerted a marked inhibitory effect on DNA synthesis of PC PTC1 cells (Fig. 6*C, left*). We established a mass population of several clones of PC cells stably coexpressing RET/PTC1 (PC PTC1) and Rap1(N17). Cell growth was measured by counting cells at different time points. Rap1(N17) coexpression blunted PC PTC1 cell proliferation in the absence of six hormones (Fig. 6*C, right*).

One of the well-known effects of Rap1 is its ability to induce cell adhesion to the substrate, cell-cell adhesion, cell spreading, and cell migration. This is likely mediated by its ability of promoting integrin activation (15). RET/PTC–expressing PC cells feature prominent actin bundles organized in stress fibers and this depends on the integrity of Y1062 (33). We used Texas Red X–conjugated phalloidin staining to analyze actin rearrangement in PC PTC1 cells transiently transfected with Rap1GAP, Rap1(N17), SH2CrkII, or C3GΔCAT. Representative micrographs are shown in Fig. 6*D* (*top*). As reported previously (33), PC PTC1 cells were highly adhesive to the plastic dish and formed a remarkable amount of

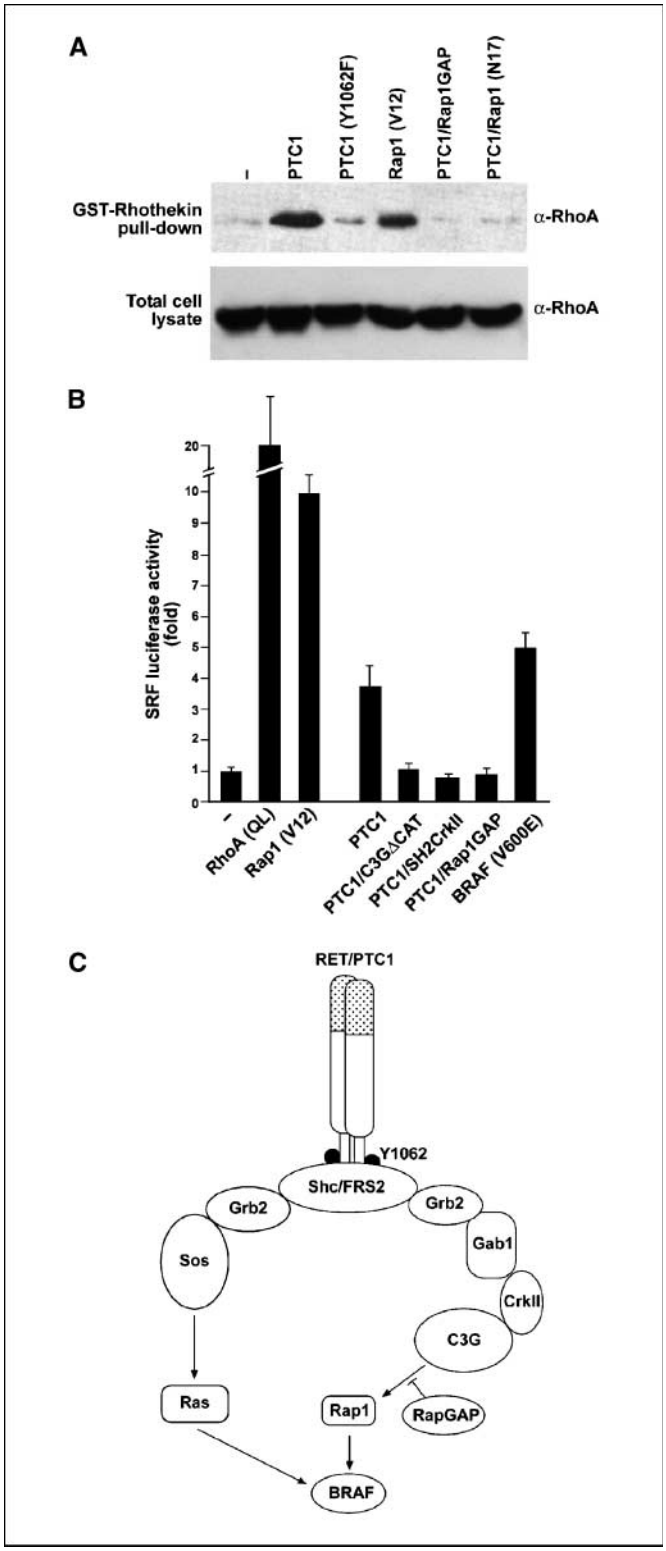

Figure 7. *A,* affinity precipitation of RhoA with GST-RhotekinGDS from cells transfected with the indicated constructs or the empty vector (−). Total RhoA levels are shown for normalization. The signal was analyzed at the PhosphorImager. This experiment is representative of three independent assays. *B,* HEK293T cells were cotransfected with pSRF-luc and the indicated plasmids. Luciferase activity was expressed as fold induction with respect to the control. *Columns,* average results of three independent determinations; *bars,* SD. *C,* Grb2 binds RET/PTC Tyr^{1062} via numerous docking proteins, including Shc and FRS2. Grb2 binds Gab1, which in turn associates to the SH2 domain of Crk. Crk via its SH3 domain bridges the complex to C3G.

stress fibers few hours (4 h) after plating. All the mutants interfering with Rap1 activation, but not the active Rap1(V12) (data not shown), inhibited stress fiber formation (Fig. 6*D, top*). PC PTC1 cells positive for stress fibers were 82.6 ± 6.7% in vector-transfected cells and 12.8 ± 4.2% ($P < 0.001$), 29.4 ± 4.2% ($P < 0.001$), 16.7 ± 3.3% ($P < 0.001$), and 30.6 ± 2.5% ($P < 0.001$) in cells transfected with Rap1GAP, Rap1(N17), SH2CrkII, or C3GΔCAT, respectively. Accordingly, PC PTC1 cells stably expressing Rap1(N17) displayed a rounded morphology and a remarkably reduced number of cells (<25%) positive for stress fibers even several days after plating (Fig. 6*D, bottom*). In contrast, PC cells stably expressing Rap1(V12) rapidly (4 h after plating) formed tick actin bundles (>65% of the cells; Fig. 6*D, bottom*). BRAF(V600E)-expressing PC cells also formed stress fibers after plating (~40% of the cells; Fig. 6*D, bottom*).

RhoA GTPase is necessary for stress fiber formation (34). RhoA activates gene transcription via the activation of the SRF (35); this is believed to be a consequence of the actin reorganization induced by RhoA (36). We measured RhoA activation by a pull-down assay with a GST-RhotekinGDS bait. In transiently transfected HEK293, RET/PTC stimulated RhoA activation and this was dependent on the integrity of Y1062 and was obstructed by Rap1GAP and Rap1(N17); Rap1(V12) stimulated RhoA as well (Fig. 7*A*). We used a luciferase reporter gene driven by tandem repeats of SRF binding elements and activated RhoA(QL) as a positive control (29). Average results ± SD are reported in Fig. 7*B*. Rap1(V12), RET/PTC1, and BRAF(V600E) stimulated pSRF-luc. For RET/PTC1, this was obstructed by the coexpression of Rap1GAP, SH2CrkII, or C3GΔCAT (Fig. 7*B*).

Discussion

In this study, we show that a large molecular complex forms on RET/PTC1 Tyr^{1062} and mediates Rap1 stimulation (Fig. 7*C*). Such a complex includes Gab1, CrkII, and C3G. In the presence of RET/PTC1, CrkII binds C3G and is recruited to Gab1. Crk proteins exist in constitutive complexes with C3G in different cell types (31) and the Crk-C3G binding can be further enhanced by Crk recruitment to membrane receptors (37, 38). By the use of dominant-negative CrkII (SH2CrkII) and C3G (C3GΔCAT) mutants, we have found that the Gab1-CrkII-C3G complex was responsible for RET/PTC1–mediated Rap1 activation. Such a molecular mechanism is similar to that described for Rap1 stimulation mediated by the Met receptor (39). Y1062 in RET/PTC is necessary for the activation of Ras and the BRAF/MAPK pathway; this in turn is essential for RET/PTC–mediated thyroid cell growth (6, 9, and 10). Here, we add further complexity to this cascade by showing that Rap1 may function in parallel with Ras by mediating the activation of BRAF and the MAPK pathway by RET/PTC.

Some phenotypical effects induced by RET/PTC1 in PC thyroid cells (e.g., mitogenesis and stress fiber formation) require Rap1 activation. Several reports show that BRAF is a key player in thyroid cell growth, as it regulates the RET/PTC–mediated MAPK activation and thyrotropin-independent proliferation (6, 9, 10). Furthermore, ~45% of human PTC feature activating mutations in BRAF (40). Therefore, it is likely that the role of Rap1 in RET/PTC–mediated thyrocyte proliferation relies on its ability of participating to BRAF stimulation. Although the mitogenic activity of Rap1 for rat thyroid cells has been described (21), it should be noted that activated Rap1 was itself insufficient to induce cell cycle entry of dog thyroid cells; therefore, it is likely that Rap1 exerts its growth-promoting ability only in conjunction with additional stimuli (22).

As far as the role of Rap1 in the actin cytoskeleton remodeling of RET/PTC–expressing PC cells, we show that this results in RhoA-mediated actin polymerization, formation of actin stress fibers, and SRF-stimulated gene transcription. It is well known that Rap1 controls, from inside the cell, activity and clustering of all integrins (β_1, β_2, and β_3 families) that are associated with the actin cytoskeleton (15). Effectors of Rap1 that act in these processes are among the others: AF-6 (a multidomain adaptor protein that binds various cell junction proteins), RapL (a small protein binding both Rap1 and integrins), Riam (a protein that binds Rap1 and induces integrin-mediated cell adhesion), Arap3 (a Rap1 effector protein that contains a RhoGAP domain), and some GEFs (Vav2 and Tiam1) for Rho family GTPases (15). Given the ability of Rap1 in stimulating cell adhesion in many cell types, it is likely that its effects on the actin cytoskeleton observed in PC PTC cells are, at least in part, indirect and mediated by stimulation of cell adhesion and spreading. However, because some of the proteins interacting with Rap1 directly modulate Rho small GTPases, a direct biochemical link between Rap1 and RhoA in RET/PTC–transformed thyrocytes could also be envisaged. This pathway (RET/PTC–Rap1-RhoA) could be distinct to that mediating BRAF and MAPK stimulation, as suggested by the notion that PC cells transformed by Ras (another potent trigger of the MAPK pathway) are negative for stress fiber formation (33). However, we also observed that PC cells expressing BRAF(V600E) contain stress fibers and BRAF has been described previously as a regulator of stress fiber formation in other cell systems (41).

Recent studies have shown that Rap1 can be implicated in tumorigenesis (14, 15) Although Rap1 mutations have not been found in human thyroid tumors (23), given the role of Rap1 in the RET/PTC signaling, it is conceivable that Rap1 or proteins involved in Rap1 signaling might be implicated in PTC tumorigenesis.

Acknowledgments

Received 3/15/2006; revised 9/21/2006; accepted 10/3/2006.

Grant support: Associazione Italiana per la Ricerca sul Cancro (AIRC) and the Italian Ministero per l'Istruzione, Università e Ricerca Scientifica (MIUR). G. De Vita and M.D. Castellone were recipient of AIRC fellowships.

The costs of publication of this article were defrayed in part by the payment of page charges. This article must therefore be hereby marked *advertisement* in accordance with 18 U.S.C. Section 1734 solely to indicate this fact.

We thank J.S. Gutkind, P.J.S. Stork, E. Santos, S. Giordano, and P. Gual for the plasmids; J.A. Fagin for the inducible RET/PTC1 cells; F. Curcio for P5 cells; F. Merolla for statistical analysis; and J.A. Gilder for text editing.

References

1. Nikiforov YE. RET/PTC rearrangement in thyroid tumors. Endocr Pathol 2002;13:3–16.
2. Fagin JA. How thyroid tumors start and why it matters: kinase mutants as targets for solid cancer pharmacotherapy. J Endocrinol 2004;183:249–56.
3. Kawamoto Y, Takeda K, Okuno Y, et al. Identification of RET autophosphorylation sites by mass spectrometry. J Biol Chem 2004;279:14213–24.
4. Asai N, Murakami H, Iwashita T, Takahashi M. A mutation at tyrosine 1062 in MEN2A-Ret and MEN2B-Ret impairs their transforming activity and association with shc adaptor proteins. J Biol Chem 1996;271:17644–9.
5. Segouffin-Cariou C, Billaud M. Transforming ability of MEN2A-RET requires activation of the phosphatidylinositol 3-kinase/AKT signaling pathway. J Biol Chem 2000;275:3568–76.
6. Melillo RM, Castellone MD, Guarino V, et al. The RET/PTC-RAS-BRAF linear signaling cascade mediates the motile and mitogenic phenotype of thyroid cancer cells. J Clin Invest 2005;115:1068–81.
7. Ichihara M, Murakumo Y, Takahashi M. RET and neuroendocrine tumors. Cancer Lett 2004;204:197–211.

8. Hayashi H, Ichihara M, Iwashita T, et al. Characterization of intracellular signals via tyrosine 1062 in RET activated by glial cell line-derived neurotrophic factor. Oncogene 2000;19:4469–75.
9. Mitsutake N, Knauf JA, Mitsutake S, Mesa C, Jr., Zhang L, Fagin JA. Conditional BRAFV600E expression induces DNA synthesis, apoptosis, dedifferentiation, and chromosomal instability in thyroid PCCL3 cells. Cancer Res 2005;65:2465–73.
10. Mitsutake N, Miyagishi M, Mitsutake S, et al. BRAF mediates RET/PTC-induced mitogen-activated protein kinase activation in thyroid cells: functional support for requirement of the RET/PTC-RAS-BRAF pathway in papillary thyroid carcinogenesis. Endocrinology 2006; 147:1014–9.
11. Besset V, Scott RP, Ibanez CF. Signaling complexes and protein-protein interactions involved in the activation of the Ras and phosphatidylinositol 3-kinase pathways by the c-Ret receptor tyrosine kinase. J Biol Chem 2000;275:39159–66.
12. De Falco V, Guarino V, Malorni L, et al. RAI(ShcC/N-Shc)-dependent recruitment of GAB 1 to RET oncoproteins potentiates PI 3-K signalling in thyroid tumors. Oncogene 2005;24:6303–13.
13. Gu H, Neel BG. The "Gab" in signal transduction. Trends Cell Biol 2003;13:122–30.
14. Stork PJ. Does Rap1 deserve a bad Rap? Trends Biochem Sci 2003;28:267–75.
15. Bos JL. Linking Rap to cell adhesion. Curr Opin Cell Biol 2005;17:123–8.
16. Kitayama H, Sugimoto Y, Matsuzaki T, Ikawa Y, Noda M. A ras-related gene with transformation suppressor activity. Cell 1989;56:77–84.
17. Vossler MR, Yao H, York RD, Pan MG, Rim CS, Stork PJ. cAMP activates MAP kinase and Elk-1 through a B-Raf- and Rap1-dependent pathway. Cell 1997;89:73–82.
18. York RD, Yao H, Dillon T, et al. Rap1 mediates sustained MAP kinase activation induced by nerve growth factor. Nature 1998;392:622–6.
19. Mishra S, Smolik SM, Forte MA, Stork PJ. Ras-independent activation of ERK signaling via the torso receptor tyrosine kinase is mediated by Rap1. Curr Biol 2005;15:366–70.
20. Mizuchi D, Kurosu T, Kida A, et al. BCR/ABL activates Rap1 and B-Raf to stimulate the MEK/Erk signaling pathway in hematopoietic cells. Biochem Biophys Res Commun 2005;326:645–51.
21. Ribeiro-Neto F, Urbani J, Lemee N, Lou L, Altschuler DL. On the mitogenic properties of Rap1b: cAMP-induced G(1)/S entry requires activated and phosphorylated Rap1b. Proc Natl Acad Sci U S A 2002;99:5418–23.
22. Dremier S, Vandeput F, Zwartkruis FJ, Bos JL, Dumont JE, Maenhaut C. Activation of the small G protein Rap1 in dog thyroid cells by both cAMP-dependent and -independent pathways. Biochem Biophys Res Commun 2000;267:7–11.
23. Vanvooren V, Allgeier A, Nguyen M, et al. Mutation analysis of the Epac-Rap1 signaling pathway in cold thyroid follicular adenomas. Eur J Endocrinol 2001;144: 605–10.
24. Saavedra HI, Knauf JA, Shirokawa JM, et al. The RAS oncogene induces genomic instability in thyroid PCCL3 cells via the MAPK pathway. Oncogene 2000;19:3948–54.
25. Vitagliano D, Carlomagno F, Motti ML, et al. Regulation of p27Kip1 protein levels contributes to mitogenic effects of the RET/PTC kinase in thyroid carcinoma cells. Cancer Res 2004;64:3823–9.
26. Guerrero C, Fernandez-Medarde A, Rojas JM, Font de Mora J, Esteban LM, Santos E. Transformation suppressor activity of C3G is independent of its CDC25-homology domain. Oncogene 1998;16:613–24.
27. Gual P, Giordano S, Anguissola S, Comoglio PM. Differential requirement of the last C-terminal tail of Met receptor for cell transformation and invasiveness. Oncogene 2001;20:5493–502.
28. Servitja JM, Masgrau R, Pardo R, et al. Metabotropic glutamate receptors activate phospholipase D in astrocytes through a protein kinase C-dependent and Rho-independent pathway. Neuropharmacology 2003;44: 171–80.
29. Marinissen MJ, Chiariello M, Tanos T, Bernard O, Narumiya S, Gutkind JS. The small GTP-binding protein RhoA regulates c-jun by a ROCK-JNK signaling axis. Mol Cell 2004;14:29–41.
30. Jin ZG, Wong C, Wu J, Berk BC. Flow shear stress stimulates Gab1 tyrosine phosphorylation to mediate protein kinase B and endothelial nitric-oxide synthase activation in endothelial cells. J Biol Chem 2005;280: 12305–9.
31. Feller SM. Crk family adaptors-signalling complex formation and biological roles. Oncogene 2001;20: 6348–71.
32. Kao S, Jaiswal RK, Kolch W, Landreth GE. Identification of the mechanisms regulating the differential activation of the mapk cascade by epidermal growth factor and nerve growth factor in PC12 cells. J Biol Chem 2001;276:18169–77.
33. Barone MV, Sepe L, Melillo RM, et al. RET/PTC1 oncogene signaling in PC Cl 3 thyroid cells requires the small GTP-binding protein Rho. Oncogene 2001;20: 6973–82.
34. Ridley AJ, Hall A. The small GTP-binding protein rho regulates the assembly of focal adhesions and actin stress fibers in response to growth factors. Cell 1992;70:389–99.
35. Hill CS, Wynne J, Treisman R. The Rho family GTPases RhoA, Rac1, and CDC42Hs regulate transcriptional activation by SRF. Cell 1995;81:1159–70.
36. Sotiropoulos A, Gineitis D, Copeland J, Treisman R. Signal-regulated activation of serum response factor is mediated by changes in actin dynamics. Cell 1999;98: 159–69.
37. Okada S, Matsuda M, Anafi M, Pawson T, Pessin JE. Insulin regulates the dynamic balance between Ras and Rap1 signaling by coordinating the assembly states of the Grb2-SOS and CrkII-C3G complexes. EMBO J 1998; 17:2554–65.
38. Ichiba T, Hashimoto Y, Nakaya M, et al. Activation of C3G guanine nucleotide exchange factor for Rap1 by phosphorylation of tyrosine 504. J Biol Chem 1999;274: 14376–81.
39. Sakkab D, Lewitzky M, Posern G, et al. Signaling of hepatocyte growth factor/scatter factor (HGF) to the small GTPase Rap1 via the large docking protein Gab1 and the adapter protein CRKL. J Biol Chem 2000;275: 10772–8.
40. Xing M. BRAF mutation in thyroid cancer. Endocr Relat Cancer 2005;12:245–62.
41. Pritchard CA, Hayes L, Wojnowski L, Zimmer A, Marais RM, Norman JC. B-Raf acts via the ROCKII/LIMK/cofilin pathway to maintain actin stress fibers in fibroblasts. Mol Cell Biol 2004;24:5937–52.